A 6D interferometric inertial isolation system

Mow-Lowry, Conor M.; Martynov, Denis

DOI:
10.1088/1361-6382/ab4e01

Document Version
Peer reviewed version

Citation for published version (Harvard):
Mow-Lowry, CM & Martynov, D 2019, 'A 6D interferometric inertial isolation system', *Classical and Quantum Gravity*, vol. 36, no. 24, 245006. https://doi.org/10.1088/1361-6382/ab4e01

A 6D interferometric inertial isolation system

A 6D interferometric inertial isolation system

C M Mow-Lowry[1] and D Martynov[1,2]

[1] School of Physics and Astronomy and Institute for Gravitational Wave Astronomy, University of Birmingham, Edgbaston, Birmingham B15 2TT, United Kingdom
[2] LIGO, Massachusetts Institute of Technology, Cambridge, Massachusetts 02139, USA

E-mail: c.m.mow-lowry@bham.ac.uk

Abstract. We present the conceptual design and noise analysis of a novel inertial-isolation scheme based on six degree-of-freedom (6D) interferometric sensing of a single reference mass. It is capable of reducing inertial motion by more than two orders of magnitude at 100 mHz compared with what is achievable with state-of-the-art seismometers. This will enable substantial improvements in the low-frequency sensitivity of gravitational-wave detectors. The scheme is inherently two-stage, the reference mass is softly suspended within the platform to be isolated, which is itself suspended from the ground. The platform is held constant relative to the reference mass and this closed-loop control effectively transfers the low acceleration-noise of the reference mass to the platform. The loop gain also reduces non-linear couplings and dynamic range requirements in the soft-suspension mechanics and the interferometric sensing.

PACS numbers: 04.80.Nn, 07.10.Fq

Gravitational waves (GW) from black hole and neutron star binaries have recently been observed by the LIGO and Virgo detectors [1–4]. These interferometers were designed to be sensitive to gravitational waves in the frequency range from 10 Hz up to a few kHz. The low frequency band (< 30 Hz) is particularly important for studying intermediate mass black holes, with masses of $\sim 10^3 M_\odot$, and for accumulating signal-to-noise ratio from lighter sources. However, during the first science runs of the Advanced LIGO and VIRGO network the signal was mostly accumulated between 30 and 300 Hz, and the observed black hole masses were from 7 to 80 $M_\odot$. Despite the sophistication and successful operation of LIGO's internal seismic isolation systems [5–7], the sensitivity of the detector degrades at low frequencies due to non-stationary control noises [8].

If no new technology is developed, future GW observatories will face similar problems. A recent paper (and supplemental material) analysed the critical noise-couplings and the upgrades required to allow astrophysically interesting sensitivity at frequencies below 10 Hz [9]. The conclusion is that the scientific returns are substantial, supported by studies of future facilities such as the Einstein Telescope [10] and Cosmic Explorer [11]. The study of low frequency noises [9] in the detectors set requirements for the inertial sensors to enable GW observations below 10 Hz. In this paper we analyse a 6D interferometric inertial isolation system and show that it has a potential to outperform the existing state-of-the-art seismometers and to satisty the requirements from [9].

Although it is designed for GW detectors, the calculated inertial isolation performance of the proposed isolation system is directly applicable to other instruments. The predicted inertial translation is substantially below that of seismically-stable bedrock, to a level of approximately $1\,\mathrm{nm}/\sqrt{\mathrm{Hz}}$ at 0.1 Hz. This is required for torsion-bar gravitational-antennae [12–14], and can reduce aliased-noise and Doppler-shifting in atom-interferometer instruments such as MIGA [15]. A range of other laboratory experiments can also benefit from such a low acceleration environment, from space-borne accelerometer development [16], to measurements of small forces such as inverse-square-law tests [17].

The novel design concept, shown in Figure 1, addresses three of the most challenging problems in terrestrial low-frequency inertial isolation: sensing and force noise of the reference mass, dynamic range, and cross-couplings between different degrees of freedom, in particular tilt-to-horizontal coupling. This is achieved by, first, employing low-noise interferometric sensors, an ultra-high-quality suspension system, and a high-vacuum enclosure. Second, the tilting resonances are set below 10 mHz to allow precise measurement of the tilt motion of the isolation platform above this frequency. Third, all six degrees of freedom are similarly quiet, such that cross-coupling doesn't spoil the performance. Finally, a high-gain control system suppresses actuation noise and dynamic range requirements in both the soft suspension and the sensing interferometers.

The central reference mass is suspended such that the weakest possible restoring forces, limited only by material properties and geometric constraints, are applied in all degrees of freedom. It is sensed by six interferometers and high-gain control holds their

outputs constant such that the isolated platform is fixed relative to the reference mass to a resolution limited by sensing noise. This process is comparable to the drag-free control successfully employed in LISA Pathfinder [18], where the spacecraft was manoeuvred around one reference mass, while a second mass was weakly constrained with electrostatic actuators. A key concept in both our proposed 6D isolator and LISA pathfinder is that all six degrees of freedom are simultaneously low-noise, all but eliminating the cross-coupling.

1. Low-frequency inertial isolation

The primary limitation of low-frequency inertial isolation systems is tilt-to-horizontal coupling [19]. The best active system is currently LIGO's ISI, which measures inertial tilt by subtracting the vertical outputs of horizontally separated sensors such as Trillium T-240 seismometers. The angular inertial performance is approximately the same as the seismometer self-noise, but it couples to the horizontal degree of freedom with a factor of g/ω^2, where g is local gravitational acceleration and ω is angular frequency [19]. This coupling factor makes the horizontal sensitivity of the seismometers worse compared to the horizontal ground motion below approximately 70 mHz.

The resulting noise prevents LIGO from significantly reducing the RMS motion of the ground at micro-seismic frequencies, $\sim 0.1 - 0.2$ Hz. Moreover, the platform motion is amplified between 10 and 70 mHz. The residual platform motion causes angular fluctuations of the test masses with an RMS amplitude of 0.1 μrad. To stabilise the motion of the laser beams on the mirrors, LIGO needs to reduce angular fluctuations of the test masses to less than 0.1% of the divergence angle of the 4-km cavities which is approximately 30 urad. This goal is achieved using wavefront-sensors [20] with a control bandwidth of a few Hz [21]. The self-noise of these wavefront-sensors is $10^{-14}\,\mathrm{rad}/\sqrt{\mathrm{Hz}}$,

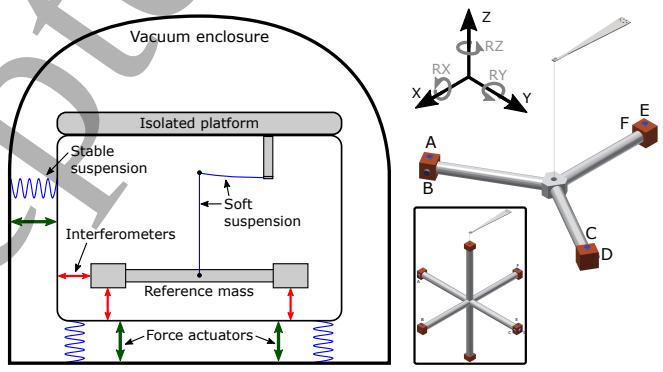

Figure 1. A 2-d representation of the isolation architecture (left) and a design concept for the reference mass and suspension (right). The pendulum length is 1 m, and the reference mass has a radius of 0.5 m and a mass of 3.8 kg. Letters indicate interferometric sensing locations. Inset right: an alternative configuration with equal moments of inertia in the three principal axes that reduces Newtonian noise in RX and RY at the expense of size and complexity.

and the angular controls degrade LIGO's sensitivity all the way up to 20-30 Hz [8].

Two approaches are currently being explored in the LIGO-Virgo collaboration to reduce low-frequency tilt-coupling. The first aims to develop a seismometer that is insensitive to tilt in a particular frequency band [22, 23]. The second aims to actively stabilize the tilt-motion of the isolated platforms using 1D rotation sensors. Custom-built devices with considerably lower self-noise than commercial seismometers have already been installed outside the vacuum system at LIGO [24, 25].

Our proposed 6D system has clear advantages over other approaches; it requires a single reference mass to stabilize a platform in all degrees of freedom, and all mechanical degrees of freedom of the mass are weakly constrained. Therefore, the cross-couplings and non-linearities are suppressed in the proposed isolation system. We note that suspending and tuning a single mass that is very soft in all three angular degrees of freedom will present significant experimental challenges. We will exploit the overlap with 1D rotation sensors and torsion-bar antennae - optically sensed large-moment reference masses - and apply similar solutions for dealing with large long-term drifts and centre-of-mass tuning.

2. Mechanical design of the reference mass

The key feature of the mechanical design is the suspension of a large-moment reference mass from a single fused-silica suspension wire. The combination of low-loss, high-strength material, and a large-moment reference mass is required to reduce the rotational thermal noise enough to allow for a transformational reduction in inertial translation at 0.1 Hz. The large tilt-measurement baseline and high precision interferometric sensing are also required to improve the resolution of the rotation readout.

We propose to suspend the reference mass from a single quasi-monolithic fused-silica fibre [26, 27], similar to the LIGO and Virgo test mass suspensions, which implies that the fibre attachments do not significantly increase the thermal noise of the mass. High performance in the tilting degrees of freedom (RX and RY as seen in Fig. 1) is crucial due to tilt-to-horizontal coupling. The tilt-modes must have very low resonant frequencies to distinguish them from translational motion and reduce sensing noise which couples to the horizontal sensitivity as $1/\omega^4$ at frequencies below the tilt resonance.

In our design these criteria are met by combining a large reference mass, a thin, highly-stressed fused silica suspension, and interferometric sensing. The three-spoked design in Fig. 1 meets these requirements.

Weakly constrained mechanical oscillators are prone to long-term drift. To keep the reference mass at its operating point and actively damp the resonant modes, low-frequency control forces must be applied. The magnitude of the required force is dependent on residual stresses and creep in the suspension materials. To prevent the applied forces from spoiling the isolation performance, we anticipate applying a combination of low-force capacitive actuation at frequencies near mechanical modes of the inertial mass, with a dynamic range of $\sim 10^6$, and step-wise re-adjustment, either

Resonances	**Frequency**	**Q**
X, Y	0.5 Hz	$>10^6$
Z	1 Hz	10^3
RX, RY	5 mHz	10^5
RZ	0.4 mHz	10^6

Table 1. Fundamental resonant frequencies and quality factors of the reference mass suspension.

manually or via slip-stick actuation. A precise control scheme of the inertial mass is a topic of the future research.

In the vertical (Z) direction a standard metal blade-spring provides compliance and supports the total mass load [28]. It might be possible to employ a lower-loss material, but in keeping with other conservative assumptions, we assume that a maraging steel blade will be used, with ∼1000 times larger loss than fused silica.

The fundamental resonant frequencies and quality factors of the six principal modes are shown in Table 1. The horizontal translational (X and Y) degrees of freedom are essentially pendulum modes. The vertical (Z) resonance is dominated by the elastic compliance of the blade spring, and the torsion (RZ) by the shear restoring torque of the fibre. The material loss angle of the fibre, ϕ_{mat}, dominated by surface and thermo-elastic loss, is conservatively assumed to be 10^{-6} [29]. A fuller description of the assumed material properties and suspension stiffnesses is given in the supplemental material.

The tilt-mode stiffnesses are affected by both elastic and gravitational restoring terms. Assuming the elastic bending length is much shorter than the pendulum length, the elastic angular stiffness of the bending fibre, κ_{el}, can be calculated as shown in [30] (and more generally as shown in [31]) resulting in

$$\kappa_{\mathrm{el}} = \frac{1}{2}\sqrt{mgEI_{\mathrm{a}}}, \tag{1}$$

where mg is the tension in the fibre, E is the elastic modulus, and I_{a} is the second moment of area, given by $I_{\mathrm{a}} = \frac{\pi}{4}r^4$ for a circular cross-section fibre of radius r.

For the parameters chosen here, the elastic resonant frequency in tilt is $\omega_{\mathrm{el}} = 2\pi \times 23\,\mathrm{mHz}$. The inertial-equivalent sensing noise rises with $1/\omega^2$ below this frequency, as seen in Fig. 2 (top). The proposed resonant frequency of $\omega_{\mathrm{RX}} = 2\pi \times 5\,\mathrm{mHz}$ was chosen to be low enough such that sensing noise in tilt does not degrade translational performance near the blending frequency of ∼10 mHz. Therefore, the centre of rotation should be between 180 and 190 μm below the centre of mass, resulting in a resonant frequency between 4 and 7 mHz. Tuning of the centre of mass relative to the centre of rotation with micron-level precision has been demonstrated, with stable long-term performance, in 1D rotation sensors with comparable mass and moment of inertia [24].

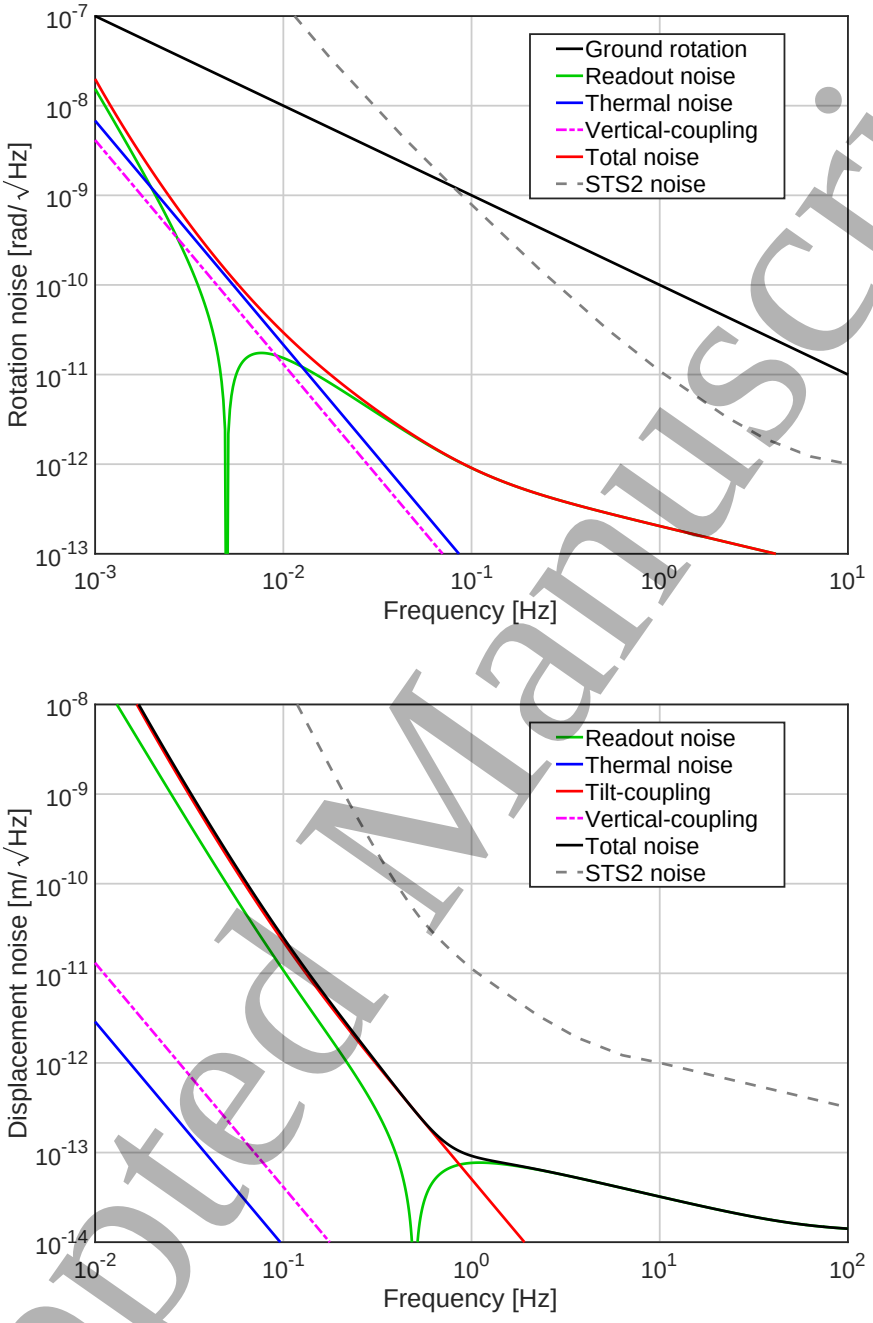

Figure 2. Sensitivity noise budgets for the angular (top) and longitudinal (bottom) degrees of freedom of the platform with the proposed isolation scheme.

3. Sensitivity analysis

We compare the performance of our 6D isolation system with the best commercial seismometers, showing that a substantial reduction of platform motion at LIGO is possible, in turn reducing the required bandwidth of auxiliary control loops by a factor of approximately 5. The predicted performance of the isolation system is limited by several noise sources, and we present an analysis of the dominant noise terms, including contributions from thermal noise of the suspension, sensing noise, temperature gradients, control noise, cross-coupling, and input ground motion.

Since tilt-to-horizontal coupling is the dominant factor in low-frequency horizontal performance, Fig. 2 shows a noise analysis of both tilt (RX, RY) and horizontal (X, Y) degrees of freedom. The STS-2 horizontal noise is shown after the subtraction of the tilt motion. This degree of freedom is measured using three STS-2 seismometers which are horizontally separated by 1 m. Cancellation of the tilt noise increases the horizontal noise by a factor of $\sqrt{1+g^2/\omega^4}$ since the horizontal and vertical noises of STS-2 are incoherent. The dominant noise source of the 6D seismometer at nearly all frequencies is the sensing noise of the proposed interferometers and thermal noise of the suspended inertial mass. The key noise terms are described below.

The input ground rotation must be strongly suppressed by closed-loop control. The 'ground rotation' trace in Fig. 1 (left) is a crude fit based on measurements made at the LIGO observatories, with a typical $1/\omega$ slope and a value of $1\,\mathrm{nrad}/\sqrt{\mathrm{Hz}}$ at 0.1 Hz. An aggressive blending frequency is used to provide strong isolation at 10 mHz.

The reference mass is sensed using 3 horizontal and 3 vertical Michelson-type interferometers at locations marked with capital letters in Fig. 1 (right). We assume that the interferometers are of the kind, and with sensitivity, recently reported in [32]. The noise is dominated by the analogue input noise of the ADC system above 0.1 Hz, and by temperature and air-pressure fluctuations at lower frequencies. Significant sensitivity gains can be expected through a combination of environmental and electronic improvements before reaching shot noise, which is $\sim 10^{-15}\,\mathrm{m}/\sqrt{\mathrm{Hz}}$ for a few milliwatts of power. In the analysis shown here a stick-figure fit is made to the reported sensitivity curve assuming no improvements are made.

The power spectral density of the thermal-noise torque applied by the bottom hinge to the reference mass is determined by the real part of the mechanical impedance

$$S_{\mathrm{torq}}(\omega) = 4k_{\mathrm{B}}T\mathrm{Re}(Z(\omega)) = 4k_{\mathrm{B}}T\phi_{\mathrm{eff}}\kappa_{\mathrm{el}}/\omega, \tag{2}$$

where k_{B} is Boltzmann's constant, T is the temperature in kelvin, and ϕ_{eff} is the effective loss angle of the oscillator. The relation between the effective loss angle and the material loss angle is dependent on the geometry of the spring, and in this case $\phi_{\mathrm{eff}} = \phi_{\mathrm{mat}}/2$ [30]. The supplemental material contains some further discussion concerning the thermal-noise torque.

All thermal noise curves are calculated assuming that the loss angles of the fibre and blade-spring are frequency independent. We assume that the loss angle of the fibre is greater than the measured loss at the thermo-elastic loss peak [29], allowing

some margin to account for the (small) anticipated clamping losses at the metal-glass interfaces.

By design, our 6D seismometer is quiet in all degrees of freedom - the high-gain control system will reduce motion down to our noise limits below a few hertz. This means that cross-coupling, typically a major problem for soft mechanical systems, is all but eliminated as an issue. Additionally, the force-noise, including actuator noise and thermal noise, of the 'stable isolation' are actively suppressed by the loop gain, and have a negligible impact on the sensitivity.

What remains important is the fundamental tilt-to-horizontal coupling, where we assume that the final inertially-controlled residual rotation shown in Fig. 2 (top) couples with g/ω^2 into horizontal translation, and coupling from the (relatively) noisy vertical (Z) direction. Fortunately, the cross-coupling between vertical and other degrees of freedom is small, and we assume a factor of 10^{-3} from thermally-driven vertical motion into horizontal and tilt motion, consistent with Advanced LIGO suspension modelling [26]. Should it prove necessary, the weak electro-static actuators can be used to fine-tune the reference mass alignment to minimize this coupling. For the analysis presented here, the maximum actuation strength is determined by the most stringent force noise requirement. This will naturally limit the control authority. The full implications of the control scheme will be studied in detail in future research.

Thermal expansion makes two distant points of the platform move differentially. We stabilize motion at one point of the isolated platform while the optic is suspended from a different location. We estimate the amplitude spectral density of the thermal-expansion-driven motion, $\sqrt{S_{\mathrm{te}}}$, of the optic suspension point at 1 mHz to be

$$\sqrt{S_{\mathrm{te}}} \approx 2 \cdot \alpha \sqrt{S_T} \Delta L = 10^{-9} \frac{\Delta T}{1\,\mathrm{mK}} \frac{\Delta L}{10\,\mathrm{cm}} \frac{\mathrm{m}}{\sqrt{\mathrm{Hz}}}, \tag{3}$$

where $\alpha \approx 2 \cdot 10^{-5}$ is the approximate coefficient of thermal expansion of aluminium, S_T is the power spectrum density of the temperature fluctuation, and ΔL is the distance between the optic suspension point and the seismometer. The temperature gradients that cause this relative motion decrease in magnitude as $1/f$ and they are additionally low-pass filtered by LIGO's vacuum enclosure with a timescale of ∼5 hours. Therefore, above 1 mHz this noise decreases as $1/f^2$ and should not limit isolation performance.

An estimate was made for the impact of Newtonian noise, but this is expected to be negligible across the frequency band of interest.

During the sensitivity analysis, we have attempted to employ conservative performance estimates where possible. The quality factor of fused silica suspension fibres has been observed in all-glass and glass-metal systems at the level indicated. Cross-coupling from the noisy vertical (Z) into the crucial tilt (RX, RY) degrees of freedom is assumed at a reasonable level, even though there is no expected linear coupling. The interferometric sensing noise performance has already been demonstrated, and improvements in that performance can be expected at low frequencies. However, what remains untested is achieving (nearly) suspension thermal-noise limited performance at very low frequencies with a reference mass with such a large moment of inertia when

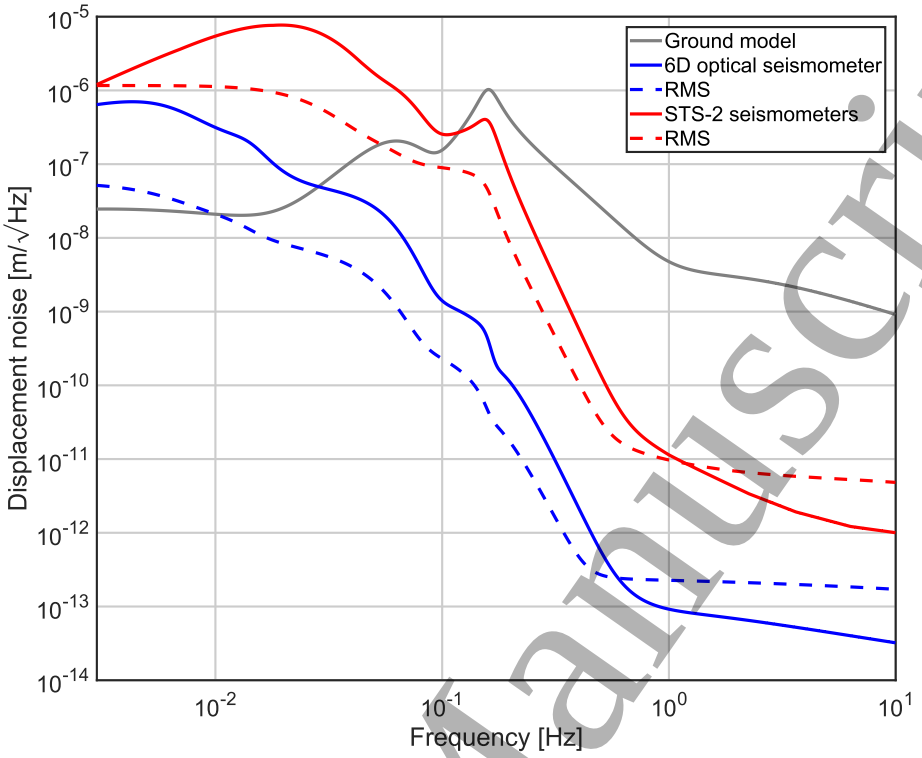

Figure 3. A comparison of the residual motion using STS-2 seismometers and the proposed 6D seismometer.

compared with existing small-force torsion balance experiments. A detailed technical study combined with experimental demonstration will be required to demonstrate the system's practical feasibility.

4. Isolation performance and impact

The '6D optical seismometer' trace in Fig. 3 represents the total inertial motion in the horizontal direction when all control loops are closed. To avoid adding low-frequency inertial sensing noise to the platform, the feedback signals are blended with position sensor signals at ∼10 mHz, effectively 'locking' the platform to the ground at very low frequencies. At higher frequencies, ground motion leaks through the blending filters (shown in the supplemental material), reducing performance near 0.1 Hz.

The predicted performance shown is more than two orders of magnitude better than what is possible with state of the art STS-2 seismometers. The RMS displacement is significantly less than a nanometre for all frequencies above 100 mHz. Such isolation will drastically simplify the lock acquisition procedure of gravitational wave detectors, which currently suffer from large low-frequency motion of ∼100 nm over 100 seconds.

During the first science runs, the coincident duty cycle of the two Advanced LIGO instruments was 44%, and each interferometer was in 'observation mode' 66% of the time. For 18% of the run, each instrument was not observing due to ground motion at micro-seismic frequencies, wind, and (small) earthquakes. Assuming that the 6D

isolation system enables operation in the presence of this elevated motion, the individual instrument duty cycle could be 81%, in turn increasing the coincident observation time to 66%. We note that the Virgo detector already achieves a duty cycle of 80% without the proposed 6D seismometer. Virgo's seismic isolation system differs from the LIGO's, for example, the Virgo suspensions are 8 m long [33] compared with ≈ 1.6 m in LIGO.

Noise from auxiliary degrees of freedom currently limits the performance of Advanced LIGO performance below 20-30 Hz [8]. The dominant contribution is from angular control of the test masses, where a closed-loop bandwidth of 2.5 Hz is required to suppress the angular motion to a few nanoradians RMS. With our proposed seismometer, the bandwidth of the auxiliary control loops will be reduced to 0.5 Hz, rendering control noise from these degrees of freedom insignificant for the gravitational wave readout above 5 Hz.

Finally, the proposed seismometer opens a way towards detecting GWs at 5 Hz using ground based detectors. Potential upgrades for the LIGO instruments have recently been proposed [9], and a 6D seismometer is a necessary but not sufficient component. A second required element is much improved local sensors for damping of the main suspension chain, and the interferometers proposed here also meet that requirement. The supplemental material in that paper addresses the performance impact (and requirements) for several proposed upgrades. There is no guarantee that eliminating the low-frequency noise sources that currently limit gravitational-wave detectors will allow astrophysically relevant sensitivity below 10 Hz, but the kind of isolation presented here is necessary even if it is not sufficient.

The rich scientific rewards for low-frequency sensitivity, including the detection of intermediate mass black holes up to $2000 M_\odot$, studies at cosmological distances of $z \approx 6$, and the possibility of pre-merger alerts for neutron star coalescence [34], demand that serious effort is made to address known limitations.

Acknowledgements — The authors wish to thank K. Venkateswara, V. Frolov, G. Hammond, B. Lantz, C.C. Speake, J. Harms, A. Freise, and R. Mittelman for useful discussions and advice. C. M-L has received funding from the European Union's Horizon 2020 research and innovation programme under the Marie Sklodowska-Curie grant agreement No 701264. D.M. is supported by the Kavli Foundation.

Appendix A. Equations of motion

The equations of motion for the reference mass and suspension are simple in Z and RZ, where only the elastic bending of the blade-spring and the torsional compliance of the suspension fibre (respectively) contribute restoring forces. The X and RY (and similarly Y and RX) degrees of freedom are intrinsically coupled. Fig. A1 shows a schematic view of the relevant parameters for determining the Lagrangian of the generalized coordinates α and β, which are approximately equal to the final Cartesian coordinates X and RY (or Y and RX). The design parameters for the reference mass and its suspension are shown in Table A1.

The flexing of the suspension fibre provides an elastic restoring torque a distance of $L_{\rm el}$ from its attachment point with an angular spring $\kappa_{\rm el}$. The displacement d between the centre of mass and the lower bending point of the fibre can be adjusted to be positive or negative (through the use of a lockable moving mass) to tune the resonant frequencies of the tilting modes. The 2-D Lagrangian is

$$\mathfrak{L} \approx \frac{mL^2}{2}\dot{\alpha}^2 + mLd\dot{\alpha}\dot{\beta} + \frac{I_{\rm RY}}{2}\dot{\beta}^2 - \frac{mgL}{2}\alpha^2 - \frac{mgd}{2}\beta^2 - \kappa_{\rm el}\alpha^2 + \kappa_{\rm el}\alpha\beta - \frac{\kappa_{\rm el}}{2}\beta^2, \tag{A.1}$$

which is valid for $d \ll L, R$ and $\alpha, \beta \ll 1$.

From the Lagrangian, the (coupled) equations of motion are derived and solved,

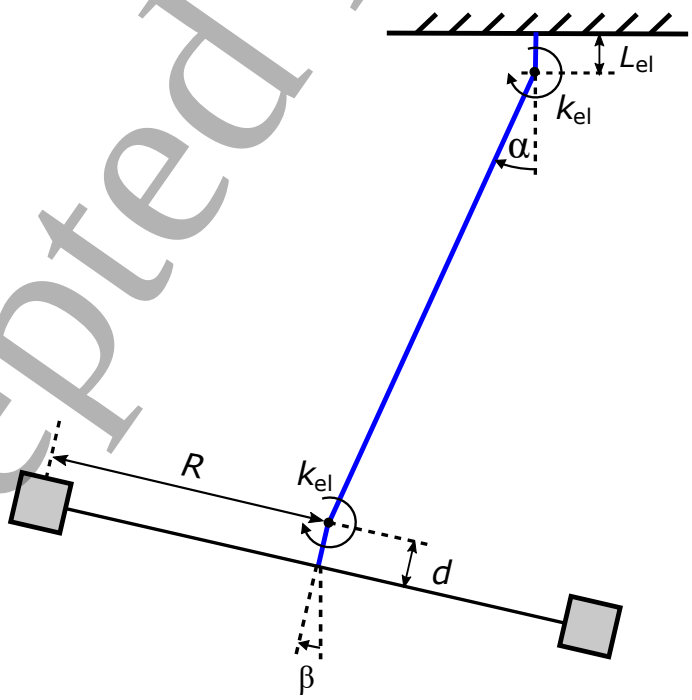

Figure A1. A simplified schematic for calculating the equations of motion in the coupled degrees of freedom. The pendulum is of length L and the reference mass has a total mass m and a moment of inertia of $I_{\rm RX}$ ($= I_{\rm RY}$).

Design property	**Value**
Suspended mass	3.8 kg
Moments of inertia ($I_{\mathrm{RX}}, I_{\mathrm{RY}}$)	0.36 kg m^2
Moment of inertia (I_{RZ})	0.72 kg m^2
Width (R)	0.5 m
Pendulum length	1 m
Vertical spring extension (Δz)	0.25 m
Fused-silica suspension fibre properties	
Elastic modulus (E)	72 GPa
Shear modulus (S)	15-25 GPa
Diameter	200 μm
Fibre stress	1200 MPa
Material loss angle (ϕ)	$< 10^{-6}$

Table A1. Design parameters of the reference mass and its suspension.

creating a stiffness matrix. From this the normal-mode frequencies can be determined as a function of the design parameters, although in practice the design height d is adjusted to give the desired resonant frequency in RX and RY.

There are limits to how much the tilt-resonances can be lowered in frequency, since such spring-antispring systems are prone to hysteresis and collapse when the quality factor approaches 0.5 [35]. Ellipticity in the suspension fibre will also make one axis stiffer than the other. However, for the parameters suggested here, neither of these issues are expected to be significant and there is still margin to reduce the total suspended mass (and as such the fibre diameter), resulting in lower elastic (tilt) resonant frequencies.

Tuning the resonant frequency down, or applying a gravitational anti-spring, 'concentrates' the elastic loss, reducing the resulting quality factor like $\omega_{\mathrm{el}}^2/\omega_{\mathrm{RX}}^2$ [36]. While this might initially seem bad, the inertial-equivalent motion (or the thermal-noise torque) is only dependent on the loss, regardless of the resonant frequency, and in this case the loss is due to anelasticity in the bending of the suspension wire.

Since the sensitivity of an inertial isolation system is determined by the free response of the reference mass, the thermal noise is given by

$$\sqrt{S_{\mathrm{rot}}(\omega)} = \frac{\sqrt{S_{\mathrm{torq}}(\omega)}}{\omega^2 I_{\mathrm{RX}}}. \tag{A.2}$$

The total suspended mass and the fibre diameter may be adjusted to achieve a constant fibre stress such that $m \propto r^2$. Combining main text Eqs. 1 and 2, we find that the

thermal-noise torque is proportional to $m^{\frac{3}{4}}$, and with supplemental Eq. A.2, the resulting angular motion is proportional to $m^{-\frac{1}{4}}$, as long as the effective radius does not change with mass.

This weak dependence of thermal noise on the suspended mass means that technical considerations can dictate the design, at the factor of a few level, rather than the elastic resonant frequency or the final quality factor of the RX and RY resonances. The size of the mass, R, is chosen such that the rotational thermal noise (barely) limits the final longitudinal inertial sensitivity. It can be readily shown that a steel or tungsten wire would have approximately two orders of magnitude worse performance thermal noise performance, and as such unable to produce satisfactory inertial isolation in this 6D system.

While the coupled equations of motion are important for the tilting modes, the fundamental horizontal translation resonances are nearly unaffected by the bottom hinge and material stiffness, and can be well approximated by a simple pendulum. Z and RZ are essentially independent of other degrees of freedom and the fundamental resonant frequencies can be, respectively, determined by the (effective) extension of the blade spring, Δz, and the torsional stiffness of the suspension wire

$$\omega_{\mathrm{X,Y}}^2 = \frac{g}{L}, \tag{A.3}$$

$$\omega_{\mathrm{Z}}^2 = \frac{g}{\Delta z}, \tag{A.4}$$

$$\omega_{\mathrm{RZ}}^2 = \frac{SJ}{LI_{\mathrm{RZ}}}, \tag{A.5}$$

where $J = \frac{\pi r^4}{2}$ is the second moment of area of the cylindrical fibre along it's long-axis.

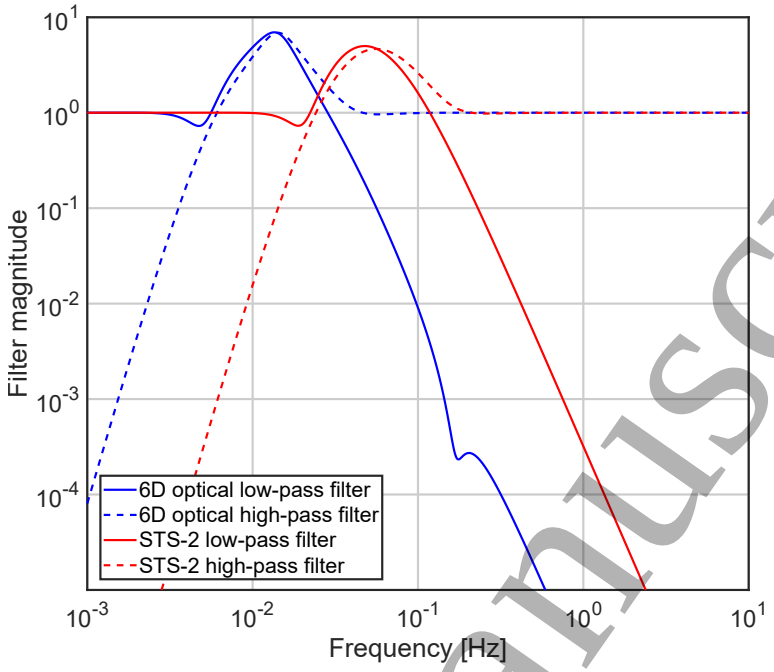

Figure B1. Blend filters for 6D and STS-2 seismometers. Signals from position sensors are used below the blending frequency for feedback control, thereby coupling the platform to the ground.

Appendix B. Sensor blending filters

At low frequencies the sensitivity of LIGO's inertial sensors degrades as $\sim 1/f^{4.5} - 1/f^{5}$ as shown in main-text Fig. 2 (bottom). In order to avoid contamination of the optical bench motion with this noise, LIGO high passes signals from inertial sensors below a particular frequency. Instead, signals from position sensors that measure the relative motion between the ground and the bench with high precision are used. The sensor blending frequency is determined by the combination of ground-motion injection and seismometer noise, and for both the STS-2 and 6D optical seismometers, it is chosen to minimize the RMS velocity of the isolated platform as a result of the combination of these terms. It is possible to lower the blend frequency, improving performance at 0.1 Hz, at the expense of substantially increased low-frequency motion.

Fig. B1 shows blending filters used to calculate the residual motion of the optical bench shown in main-text Fig. 3 with the 6D seismometer (10 mHz blend) and STS-2 seismometers (40 mHz blend). In each case the low- and high-pass filters are complementary (the sum is equal to one).

Bibliography

[1] The LIGO Scientific Collaboration and The Virgo Collaboration. Observation of gravitational waves from a binary black hole merger. *Phys. Rev. Lett.*, 116:061102, Feb 2016.

[2] The LIGO Scientific Collaboration and The Virgo Collaboration. Gw151226: Observation of gravitational waves from a 22-solar-mass binary black hole coalescence. *Phys. Rev. Lett.*, 116:241103, Jun 2016.

[3] The LIGO Scientific Collaboration and The Virgo Collaboration. Gw170814: A three-detector observation of gravitational waves from a binary black hole coalescence. *Phys. Rev. Lett.*, 119:141101, Oct 2017.

[4] The LIGO Scientific Collaboration and The Virgo Collaboration. Gw170817: Observation of gravitational waves from a binary neutron star inspiral. *Phys. Rev. Lett.*, 119:161101, Oct 2017.

[5] F Matichard, B Lantz, R Mittleman, K Mason, J Kissel, B Abbott, S Biscans, J McIver, R Abbott, S Abbott, E Allwine, S Barnum, J Birch, C Celerier, D Clark, D Coyne, D DeBra, R DeRosa, M Evans, S Foley, P Fritschel, J A Giaime, C Gray, G Grabeel, J Hanson, C Hardham, M Hillard, W Hua, C Kucharczyk, M Landry, A Le Roux, V Lhuillier, D Macleod, M Macinnis, R Mitchell, B O'Reilly, D Ottaway, H Paris, A Pele, M Puma, H Radkins, C Ramet, M Robinson, L Ruet, P Sarin, D Shoemaker, A Stein, J Thomas, M Vargas, K Venkateswara, J Warner, and S Wen. Seismic isolation of advanced ligo: Review of strategy, instrumentation and performance. *Classical and Quantum Gravity*, 32(18):185003, 2015.

[6] F. Matichard, B. Lantz, K. Mason, R. Mittleman, B. Abbott, S. Abbott, E. Allwine, S. Barnum, J. Birch, S. Biscans, D. Clark, D. Coyne, D. DeBra, R. DeRosa, S. Foley, P. Fritschel, J.A. Giaime, C. Gray, G. Grabeel, J. Hanson, M. Hillard, J. Kissel, C. Kucharczyk, A. Le Roux, V. Lhuillier, M. Macinnis, B. O'Reilly, D. Ottaway, H. Paris, M. Puma, H. Radkins, C. Ramet, M. Robinson, L. Ruet, P. Sareen, D. Shoemaker, A. Stein, J. Thomas, M. Vargas, and J. Warner. Advanced LIGO two-stage twelve-axis vibration isolation and positioning platform. part 1: Design and production overview. *Precision Engineering*, 40:273 – 286, 2015.

[7] F. Matichard, B. Lantz, K. Mason, R. Mittleman, B. Abbott, S. Abbott, E. Allwine, S. Barnum, J. Birch, S. Biscans, D. Clark, D. Coyne, D. DeBra, R. DeRosa, S. Foley, P. Fritschel, J.A. Giaime, C. Gray, G. Grabeel, J. Hanson, M. Hillard, J. Kissel, C. Kucharczyk, A. Le Roux, V. Lhuillier, M. Macinnis, B. O'Reilly, D. Ottaway, H. Paris, M. Puma, H. Radkins, C. Ramet, M. Robinson, L. Ruet, P. Sareen, D. Shoemaker, A. Stein, J. Thomas, M. Vargas, and J. Warner. Advanced LIGO two-stage twelve-axis vibration isolation and positioning platform. part 2: Experimental investigation and tests results. *Precision Engineering*, 40:287 – 297, 2015.

[8] D. V. Martynov et al. Sensitivity of the advanced ligo detectors at the beginning of gravitational wave astronomy. *Phys. Rev. D*, 93:112004, Jun 2016.

[9] Hang Yu, Denis Martynov, Salvatore Vitale, Matthew Evans, David Shoemaker, Bryan Barr, Giles Hammond, Stefan Hild, James Hough, Sabina Huttner, Sheila Rowan, Borja Sorazu, Ludovico Carbone, Andreas Freise, Conor Mow-Lowry, Katherine L. Dooley, Paul Fulda, Hartmut Grote, and Daniel Sigg. Prospects for detecting gravitational waves at 5 hz with ground-based detectors. *Phys. Rev. Lett.*, 120:141102, Apr 2018.

[10] B Sathyaprakash, M Abernathy, F Acernese, P Ajith, B Allen, P Amaro-Seoane, N Andersson, S Aoudia, K Arun, P Astone, B Krishnan, L Barack, F Barone, B Barr, M Barsuglia, M Bassan, R Bassiri, M Beker, N Beveridge, M Bizouard, C Bond, S Bose, L Bosi, S Braccini, C Bradaschia, M Britzger, F Brueckner, T Bulik, H J Bulten, O Burmeister, E Calloni, P Campsie, L Carbone, G Cella, E Chalkley, E Chassande-Mottin, S Chelkowski, A Chincarini, A Di Cintio, J Clark, E Coccia, C N Colacino, J Colas, A Colla, A Corsi, A Cumming, L Cunningham, E Cuoco, S Danilishin, K Danzmann, E Daw, R De Salvo, W Del Pozzo, T Dent, R De Rosa, L Di Fiore, M Di Paolo Emilio, A Di Virgilio, A Dietz, M Doets, J Dueck, M Edwards, V Fafone, S Fairhurst, P Falferi, M Favata, V Ferrari, F Ferrini, F Fidecaro, R Flaminio, J Franc, F Frasconi, A Freise, D Friedrich, P Fulda, J Gair, M Galimberti, G Gemme, E Genin,

A Gennai, A Giazotto, K Glampedakis, S Gossan, R Gouaty, C Graef, W Graham, M Granata, H Grote, G Guidi, J Hallam, G Hammond, M Hannam, J Harms, K Haughian, I Hawke, D Heinert, M Hendry, I Heng, E Hennes, S Hild, J Hough, D Huet, S Husa, S Huttner, B Iyer, D I Jones, G Jones, I Kamaretsos, C Kant Mishra, F Kawazoe, F Khalili, B Kley, K Kokeyama, K Kokkotas, S Kroker, R Kumar, K Kuroda, B Lagrange, N Lastzka, T G F Li, M Lorenzini, G Losurdo, H Lück, E Majorana, V Malvezzi, I Mandel, V Mandic, S Marka, F Marin, F Marion, J Marque, I Martin, D Mc Leod, D Mckechan, M Mehmet, C Michel, Y Minenkov, N Morgado, A Morgia, S Mosca, L Moscatelli, B Mours, H Müller-Ebhardt, P Murray, L Naticchioni, R Nawrodt, J Nelson, R O' Shaughnessy, C D Ott, C Palomba, A Paoli, G Parguez, A Pasqualetti, R Passaquieti, D Passuello, M Perciballi, F Piergiovanni, L Pinard, M Pitkin, W Plastino, M Plissi, R Poggiani, P Popolizio, E Porter, M Prato, G Prodi, M Punturo, P Puppo, D Rabeling, I Racz, P Rapagnani, V Re, J Read, T Regimbau, H Rehbein, S Reid, F Ricci, F Richard, C Robinson, A Rocchi, R Romano, S Rowan, A Rüdiger, A Samblowski, L Santamaría, B Sassolas, R Schilling, P Schmidt, R Schnabel, B Schutz, C Schwarz, J Scott, P Seidel, A M Sintes, K Somiya, C F Sopuerta, B Sorazu, F Speirits, L Storchi, K Strain, S Strigin, P Sutton, S Tarabrin, B Taylor, A Thürin, K Tokmakov, M Tonelli, H Tournefier, R Vaccarone, H Vahlbruch, J F J van den Brand, C Van Den Broeck, S van der Putten, M van Veggel, A Vecchio, J Veitch, F Vetrano, A Vicere, S Vyatchanin, P Weßels, B Willke, W Winkler, G Woan, A Woodcraft, and K Yamamoto. Scientific objectives of einstein telescope. *Classical and Quantum Gravity*, 29(12):124013, 2012.

[11] B P Abbott, R Abbott, T D Abbott, M R Abernathy, K Ackley, C Adams, P Addesso, R X Adhikari, V B Adya, C Affeldt, N Aggarwal, O D Aguiar, A Ain, P Ajith, B Allen, P A Altin, S B Anderson, W G Anderson, K Arai, M C Araya, C C Arceneaux, J S Areeda, K G Arun, G Ashton, M Ast, S M Aston, P Aufmuth, C Aulbert, S Babak, P T Baker, S W Ballmer, J C Barayoga, S E Barclay, B C Barish, D Barker, B Barr, L Barsotti, J Bartlett, I Bartos, R Bassiri, J C Batch, C Baune, A S Bell, B K Berger, G Bergmann, C P L Berry, J Betzwieser, S Bhagwat, R Bhandare, I A Bilenko, G Billingsley, J Birch, R Birney, S Biscans, A Bisht, C Biwer, J K Blackburn, C D Blair, D G Blair, R M Blair, O Bock, C Bogan, A Bohe, C Bond, R Bork, S Bose, P R Brady, V B Braginsky, J E Brau, M Brinkmann, P Brockill, J E Broida, A F Brooks, D A Brown, D D Brown, N M Brown, S Brunett, C C Buchanan, A Buikema, A Buonanno, R L Byer, M Cabero, L Cadonati, C Cahillane, J Calderón Bustillo, T Callister, J B Camp, K C Cannon, J Cao, C D Capano, S Caride, S Caudill, M Cavaglià, C B Cepeda, S J Chamberlin, M Chan, S Chao, P Charlton, B D Cheeseboro, H Y Chen, Y Chen, C Cheng, H S Cho, M Cho, J H Chow, N Christensen, Q Chu, S Chung, G Ciani, F Clara, J A Clark, C G Collette, L Cominsky, M Constancio Jr, D Cook, T R Corbitt, N Cornish, A Corsi, C A Costa, M W Coughlin, S B Coughlin, S T Countryman, P Couvares, E E Cowan, D M Coward, M J Cowart, D C Coyne, R Coyne, K Craig, J D E Creighton, J Cripe, S G Crowder, A Cumming, L Cunningham, T Dal Canton, S L Danilishin, K Danzmann, N S Darman, A Dasgupta, C F Da Silva Costa, I Dave, G S Davies, E J Daw, S De, D DeBra, W Del Pozzo, T Denker, T Dent, V Dergachev, R T DeRosa, R DeSalvo, R C Devine, S Dhurandhar, M C Díaz, I Di Palma, F Donovan, K L Dooley, S Doravari, R Douglas, T P Downes, M Drago, R W P Drever, J C Driggers, S E Dwyer, T B Edo, M C Edwards, A Effler, H-B Eggenstein, P Ehrens, J Eichholz, S S Eikenberry, W Engels, R C Essick, T Etzel, M Evans, T M Evans, R Everett, M Factourovich, H Fair, S Fairhurst, X Fan, Q Fang, B Farr, W M Farr, M Favata, M Fays, H Fehrmann, M M Fejer, E Fenyvesi, E C Ferreira, R P Fisher, M Fletcher, Z Frei, A Freise, R Frey, P Fritschel, V V Frolov, P Fulda, M Fyffe, H A G Gabbard, J R Gair, S G Gaonkar, G Gaur, N Gehrels, P Geng, J George, L Gergely, Abhirup Ghosh, Archisman Ghosh, J A Giaime, K D Giardina, K Gill, A Glaefke, E Goetz, R Goetz, L Gondan, G González, A Gopakumar, N A Gordon, M L Gorodetsky, S E Gossan, C Graef, P B Graff, A Grant, S Gras, C Gray, A C Green, H Grote, S Grunewald, X Guo, A Gupta, M K Gupta, K E Gushwa, E K Gustafson, R Gustafson, J J Hacker, B R Hall, E D Hall, G Hammond, M Haney, M M Hanke, J Hanks, C Hanna, M D Hannam, J Hanson,

T Hardwick, G M Harry, I W Harry, M J Hart, M T Hartman, C-J Haster, K Haughian, M C Heintze, M Hendry, I S Heng, J Hennig, J Henry, A W Heptonstall, M Heurs, S Hild, D Hoak, K Holt, D E Holz, P Hopkins, J Hough, E A Houston, E J Howell, Y M Hu, S Huang, E A Huerta, B Hughey, S Husa, S H Huttner, T Huynh-Dinh, N Indik, D R Ingram, R Inta, H N Isa, M Isi, T Isogai, B R Iyer, K Izumi, H Jang, K Jani, S Jawahar, L Jian, F Jiménez-Forteza, W W Johnson, D I Jones, R Jones, L Ju, K Haris, C V Kalaghatgi, V Kalogera, S Kandhasamy, G Kang, J B Kanner, S J Kapadia, S Karki, K S Karvinen, M Kasprzack, E Katsavounidis, W Katzman, S Kaufer, T Kaur, K Kawabe, M S Kehl, D Keitel, D B Kelley, W Kells, R Kennedy, J S Key, F Y Khalili, S Khan, Z Khan, E A Khazanov, N Kijbunchoo, Chi-Woong Kim, Chunglee Kim, J Kim, K Kim, N Kim, W Kim, Y-M Kim, S J Kimbrell, E J King, P J King, J S Kissel, B Klein, L Kleybolte, S Klimenko, S M Koehlenbeck, V Kondrashov, A Kontos, M Korobko, W Z Korth, D B Kozak, V Kringel, C Krueger, G Kuehn, P Kumar, R Kumar, L Kuo, B D Lackey, M Landry, J Lange, B Lantz, P D Lasky, M Laxen, A Lazzarini, S Leavey, E O Lebigot, C H Lee, H K Lee, H M Lee, K Lee, A Lenon, J R Leong, Y Levin, J B Lewis, T G F Li, A Libson, T B Littenberg, N A Lockerbie, A L Lombardi, L T London, J E Lord, M Lormand, J D Lough, H Lück, A P Lundgren, R Lynch, Y Ma, B Machenschalk, M MacInnis, D M Macleod, F Magaña-Sandoval, L Magaña Zertuche, R M Magee, V Mandic, V Mangano, G L Mansell, M Manske, S Márka, Z Márka, A S Markosyan, E Maros, I W Martin, D V Martynov, K Mason, T J Massinger, M Masso-Reid, F Matichard, L Matone, N Mavalvala, N Mazumder, R McCarthy, D E McClelland, S McCormick, S C McGuire, G McIntyre, J McIver, D J McManus, T McRae, S T McWilliams, D Meacher, G D Meadors, A Melatos, G Mendell, R A Mercer, E L Merilh, S Meshkov, C Messenger, C Messick, P M Meyers, H Miao, H Middleton, E E Mikhailov, A L Miller, A Miller, B B Miller, J Miller, M Millhouse, J Ming, S Mirshekari, C Mishra, S Mitra, V P Mitrofanov, G Mitselmakher, R Mittleman, S R P Mohapatra, B C Moore, C J Moore, D Moraru, G Moreno, S R Morriss, K Mossavi, C M Mow-Lowry, G Mueller, A W Muir, Arunava Mukherjee, D Mukherjee, S Mukherjee, N Mukund, A Mullavey, J Mun. Exploring the sensitivity of next generation gravitational wave detectors. *Classical and Quantum Gravity*, 34(4):044001, 2017.

[12] Masaki Ando, Koji Ishidoshiro, Kazuhiro Yamamoto, Kent Yagi, Wataru Kokuyama, Kimio Tsubono, and Akiteru Takamori. Torsion-bar antenna for low-frequency gravitational-wave observations. *Phys. Rev. Lett.*, 105:161101, Oct 2010.

[13] D. J. McManus, M. J. Yap, R. L. Ward, D. A. Shaddock, D. E. McClelland, and B. J. J. Slagmolen. Torpedo: A low frequency gravitational force sensor. *Journal of Physics: Conference Series*, 716(1):012027, 2016.

[14] Tomofumi Shimoda, Naoki Aritomi, Ayaka Shoda, Yuta Michimura, and Masaki Ando. Seismic cross-coupling noise in torsion pendulums. *Phys. Rev. D*, 97:104003, May 2018.

[15] B. Canuel, A. Bertoldi, L. Amand, E. Borgo di Pozzo, B. Fang, R. Geiger, J. Gillot, S. Henry, J. Hinderer, D. Holleville, G. Lefèvre, M. Merzougui, N. Mielec, T. Monfret, S. Pelisson, M. Prevedelli, S. Reynaud, I. Riou, Y. Rogister, S. Rosat, E. Cormier, A. Landragin, W. Chaibi, S. Gaffet, and P. Bouyer. Exploring gravity with the MIGA large scale atom interferometer. *ArXiv e-prints*, 2017.

[16] Z B Zhou, L Liu, H B Tu, Y Z Bai, and J Luo. Seismic noise limit for ground-based performance measurements of an inertial sensor using a torsion balance. *Classical and Quantum Gravity*, 27(17):175012, 2010.

[17] E.G. Adelberger, B.R. Heckel, and A.E. Nelson. Tests of the gravitational inverse-square law. *Annual Review of Nuclear and Particle Science*, 53(1):77–121, 2003.

[18] M. Armano, H. Audley, G. Auger, J. T. Baird, M. Bassan, P. Binetruy, M. Born, D. Bortoluzzi, N. Brandt, M. Caleno, L. Carbone, A. Cavalleri, A. Cesarini, G. Ciani, G. Congedo, A. M. Cruise, K. Danzmann, M. de Deus Silva, R. De Rosa, M. Diaz-Aguiló, L. Di Fiore, I. Diepholz, G. Dixon, R. Dolesi, N. Dunbar, L. Ferraioli, V. Ferroni, W. Fichter, E. D. Fitzsimons, R. Flatscher, M. Freschi, A. F. García Marín, C. García Marirrodriga, R. Gerndt, L. Gesa, F. Gibert,

D. Giardini, R. Giusteri, F. Guzmán, A. Grado, C. Grimani, A. Grynagier, J. Grzymisch, I. Harrison, G. Heinzel, M. Hewitson, D. Hollington, D. Hoyland, M. Hueller, H. Inchauspé, O. Jennrich, P. Jetzer, U. Johann, B. Johlander, N. Karnesis, B. Kaune, N. Korsakova, C. J. Killow, J. A. Lobo, I. Lloro, L. Liu, J. P. López-Zaragoza, R. Maarschalkerweerd, D. Mance, V. Martín, L. Martin-Polo, J. Martino, F. Martin-Porqueras, S. Madden, I. Mateos, P. W. McNamara, J. Mendes, L. Mendes, A. Monsky, D. Nicolodi, M. Nofrarias, S. Paczkowski, M. Perreur-Lloyd, A. Petiteau, P. Pivato, E. Plagnol, P. Prat, U. Ragnit, B. Raïs, J. Ramos-Castro, J. Reiche, D. I. Robertson, H. Rozemeijer, F. Rivas, G. Russano, J. Sanjuán, P. Sarra, A. Schleicher, D. Shaul, J. Slutsky, C. F. Sopuerta, R. Stanga, F. Steier, T. Sumner, D. Texier, J. I. Thorpe, C. Trenkel, M. Tröbs, H. B. Tu, D. Vetrugno, S. Vitale, V. Wand, G. Wanner, H. Ward, C. Warren, P. J. Wass, D. Wealthy, W. J. Weber, L. Wissel, A. Wittchen, A. Zambotti, C. Zanoni, T. Ziegler, and P. Zweifel. Sub-femto-g free fall for space-based gravitational wave observatories: Lisa pathfinder results. *Phys. Rev. Lett.*, 116:231101, Jun 2016.

[19] B. Lantz, R. Schofield, B. O'Reilly, D. E. Clark, and D. DeBra. Review: Requirements for a ground rotation sensor to improve advanced ligo. *Bull. Seismol. Soc. Am.*, 99:980, 2009.

[20] L. Barsotti, M. Evans, and P. Fritschel. Alignment sensing and control in advanced LIGO. *Classical and Quantum Gravity*, 27(8):084026, April 2010.

[21] D. Martynov. *Lock Acquisition and Sensitivity Analysis of Advanced LIGO Interferometers*. PhD thesis, Caltech, 2015.

[22] F. Matichard and M. Evans. Review: Tilt-Free Low-Noise Seismometry. *The Bulletin of the Seismological Society of America*, 105:497–510, April 2015.

[23] F. Matichard, M. Evans, R. Mittleman, M. MacInnis, S. Biscans, K. L. Dooley, H. Sohier, A. Lauriero, H. Paris, J. Koch, P. Knothe, A. Carbajo, and C. Dufort. Modeling and experiment of the suspended seismometer concept for attenuating the contribution of tilt motion in horizontal measurements. *Review of Scientific Instruments*, 87(6):065002, 2016.

[24] Krishna Venkateswara, Charles A. Hagedorn, Matthew D. Turner, Trevor Arp, and Jens H. Gundlach. A high-precision mechanical absolute-rotation sensor. *Rev. Sci. Instrum.*, 85:015005, 2014.

[25] Krishna Venkateswara, Charles Hagedorn, Jens H. Gundlach, Jeffery Kissel, Jim Warner, Hugh Radkins, Thomas Shaffer, Brian Lantz, Richard Mittleman, Fabrice Matichard, and Robert Schofield. Subtracting tilt from a horizontal seismometer using a ground-rotation sensor. *Bulletin of the Seismological Society of America*, 107:709–717, 03 2017.

[26] A V Cumming, A S Bell, L Barsotti, M A Barton, G Cagnoli, D Cook, L Cunningham, M Evans, G D Hammond, G M Harry, A Heptonstall, J Hough, R Jones, R Kumar, R Mittleman, N A Robertson, S Rowan, B Shapiro, K A Strain, K Tokmakov, C Torrie, and A A van Veggel. Design and development of the advanced ligo monolithic fused silica suspension. *Classical and Quantum Gravity*, 29(3):035003, 2012.

[27] D. Aisa, S. Aisa, C. Campeggi, M. Colombini, A. Conte, L. Farnesini, E. Majorana, F. Mezzani, M. Montani, L. Naticchioni, M. Perciballi, F. Piergiovanni, A. Piluso, P. Puppo, P. Rapagnani, F. Travasso, A. Vicerè, and H. Vocca. The advanced virgo monolithic fused silica suspension. *Nuclear Instruments and Methods in Physics Research Section A: Accelerators, Spectrometers, Detectors and Associated Equipment*, 824(Supplement C):644 – 645, 2016. Frontier Detectors for Frontier Physics: Proceedings of the 13th Pisa Meeting on Advanced Detectors.

[28] M. Beccaria, M. Bernardini, S. Braccini, C. Bradaschia, G. Cagnoli, C. Casciano, G. Cella, E. Cuoco, V. Dattilo, G. De Carolis, R. De Salvo, A. Di Virgilio, G.T. Feng, I. Ferrante, F. Fidecaro, F. Frasconi, A. Gaddi, L. Gammaitoni, A. Gennai, A. Giazotto, L. Holloway, J. Kovalik, P. La Penna, G. Losurdo, S. Malik, S. Mancini, F. Marchesoni, J. Nicolas, F. Palla, H.B. Pan, F. Paoletti, A. Pasqualetti, D. Passuello, R. Poggiani, P. Popolizio, M. Punturo, F. Raffaelli, V. Rubino, R. Valentini, A. Vicere, F. Waharte, and Z. Zhang. The creep problem in the virgo suspensions: a possible solution using maraging steel. *Nuclear Instruments and Methods in Physics Research Section A: Accelerators, Spectrometers, Detectors and Associated*

Equipment, 404(2):455 – 469, 1998.

[29] A Heptonstall, M A Barton, A S Bell, A Bohn, G Cagnoli, A Cumming, A Grant, E Gustafson, G D Hammond, J Hough, R Jones, R Kumar, K Lee, I W Martin, N A Robertson, S Rowan, K A Strain, and K V Tokmakov. Enhanced characteristics of fused silica fibers using laser polishing. *Classical and Quantum Gravity*, 31(10):105006, 2014.

[30] G. Cagnoli, J. Hough, D. DeBra, M.M. Fejer, E. Gustafson, S. Rowan, and V. Mitrofanov. Damping dilution factor for a pendulum in an interferometric gravitational waves detector. *Phys. Lett. A*, 272(1):39 – 45, 2000.

[31] Clive C Speake. Anelasticity in flexure strips revisited. *Metrologia*, 2017.

[32] S J Cooper, C J Collins, A C Green, D Hoyland, C C Speake, A Freise, and C M Mow-Lowry. A compact, large-range interferometer for precision measurement and inertial sensing. *Classical and Quantum Gravity*, 35(9):095007, 2018.

[33] The VIRGO Collaboration (presented Braccini). The VIRGO suspensions. *Classical and Quantum Gravity*, 19(7):1623–1629, mar 2002.

[34] Kipp Cannon, Romain Cariou, Adrian Chapman, Mireia Crispin-Ortuzar, Nickolas Fotopoulos, Melissa Frei, Chad Hanna, Erin Kara, Drew Keppel, Laura Liao, Stephen Privitera, Antony Searle, Leo Singer, and Alan Weinstein. Toward early-warning detection of gravitational waves from compact binary coalescence. *The Astrophysical Journal*, 748(2):136, 2012.

[35] Peter R. Saulson, Robin T. Stebbins, Frank D. Dumont, and Scott E. Mock. The inverted pendulum as a probe of anelasticity. *Rev. Sci. Instrum.*, 65(1):182, 1994.

[36] J. Harms and C. M. Mow-Lowry. Suspension-thermal noise in spring-antispring systems for future gravitational-wave detectors. *Classical and Quantum Gravity*, 2017.